Sparse Spatial and Temporal Estimation for Multipath Mitigation in GNSS

Ning Chang, Wenjie Wang, Xi Hong
School of Information and Communications Engineering
Xi'an Jiaotong University
Xi'an, China
{changning@stu., wjwang@, harryhong@stu.}xjtu.edu.cn

Jose A. Lopez-Salcedo, Gonzalo Seco-Granados
Department of Telecommunications and Systems Engineering
Universitat Autonoma de Barcelona
Barcelona, Spain
{jose.salcedo, Gonzalo.Seco}@uab.cat

***Abstract*—The multipath signals will degrade the tracking performance and increase the positioning errors of the Global Navigation Satellite System (GNSS). Superior multipath mitigation can be obtained by jointly estimating the angles of arrival and delays of both the line of sight signal and the multipath signals. In to do so, this paper proposes the use of the multiple Bayesian learning (MSBL) method together with the joint angle and delay estimation technique in GNSS multipath scenarios. Moreover, to further enhance the resolution, off-grid estimation is adopted to delay while on-grid estimation is kept for angle to reduce the complexity. Simulation results are presented to evaluate the performance of the proposed joint on-grid angle and off-grid delay estimation based on MSBL algorithm under several multipath scenarios and it is shown to outperform existing methods even in the most difficult cases of spatially correlated multipath signals and low carrier-to-noise ratio.**

***Index Terms*—GNSS multipath signals, Multiple sparse Bayesian learning, Joint angle and delay estimation, off-grid estimation**

I. Introduction

The GNSS receiver is often influenced by multipath signals which will cause tracking performance degradation and positioning error increase [1]. To address these problems, the estimation of parameters for GNSS multipath signals in multi-antenna GNSS receiver has attracted a lot of attention as it can be used for the purpose of multipath mitigation [2].

Many techniques have been proposed in the literature utilizing multiple antenna for GNSS multipath parameter estimation[3]. Space-Alternating Generalized Expectation maximization (SAGE) [4-5] is based on the maximum likelihood (ML) principle and separates multipath signals and estimating parameters of each path iteratively. However, SAGE can only guarantee local optimality and its performance is extremely sensitive to initial values. Different from SAGE, subspace-based methods like multiple signal classification (MUSIC) [6] method and estimating signal parameters via rotational invariance techniques (ESPRIT) [7] are also well known. Although subspace-based methods have relatively lower computational complexity, their performance is suboptimal and ineffective for coherent signals. JADE is proposed in [8] to estimate the signal parameters by vectoring spatial and temporal data and it has been applied for GNSS multipath discrimination [9-11]. Nevertheless, it is worth pointing out that most of these methods mentioned above only work satisfactorily with signals with low spatial or temporal correlation. Moreover, such methods also face a degradation in low carrier-to-noise ratio (C/N_0).

In this paper, an alternative approach is followed by formulating the problem using a compressed sensing perspective. With this approach, the signals in a specific domain can be sparsely representative by multiple fixed grid points, then parameters could be estimated from the corresponding grid points which is also called on-grid estimation [12]. Among all the compressed sensing methods, sparse Bayesian learning (SBL) [13] and multiple sparse Bayesian learning (MSBL) [14] use a Bayesian approach together with the expectation maximization where two advantages indicate that the global minima of SBL are always the sparsest one and SBL has much few local minima. It is also robust to highly correlated signals which brings the huge advantage for distinguishing GNSS multipath signals. To immensely improve the direction-of-arrival (DOA) estimation performance without dense sampling grids, the off-grid sparse Bayesian inference method was proposed in [15].

Inspired by the above methods, the joint DOA and delay estimation problem for GNSS multipath scenario is investigated in this paper. The application of the temporally beamspaced joint spatial and temporal domain sparse model improves the multipath discrimination and increases the number of paths whose parameters can be estimated. To fully exploit the superiority of robustness against multipath signals and adaptiveness to low C/N_0 values, we proposed the combination of JADE and MSBL in a GNSS context. Besides, considering that more accuracy is required in the temporal domain than the spatial domain because the GNSS pseudorange observable is a time delay estimate, on-grid estimation is used particularly on DOA to greatly reduce the computational overhead. While for time delay, the application of off-grid estimation brings a more accurate estimate with fewer number of grids. Thus, an algorithm named joint on-grid DOA and off-grid delay estimation based on MSBL (JAODE-MSBL) is proposed.

Notation: Matrices are denoted by capital letters in boldface (e.g., $\boldsymbol{A}$), and vectors are denoted by lowercase letters in boldface (e.g., $\boldsymbol{a}$). $E\{\cdot\}$ denotes the expectation operation. $\mathcal{CN}(\boldsymbol{\mu}, \boldsymbol{\Sigma})$ denotes the complex Gaussian distribution with the mean $\boldsymbol{\mu}$ and variance $\boldsymbol{\Sigma}$. $\|\cdot\|_F^2$, $\|\cdot\|_2^2$, $\otimes$, $\odot$, $Tr\{\cdot\}$, $vec\{\cdot\}$,

978-1-7281-0244-3/20/$31.00 ©2020 IEEE

$\mathrm{diag}\{\cdot\}$, $(\cdot)^{-1}$, $(\cdot)^T$, $(\cdot)^H$ denote the Frobenius norm, the ℓ_2 norm, the Kronecker product, the Hadamard product, the trace of a matrix, the vectorization of a matrix, the diagonalization of a matrix, the inversion, the matrix transpose and the Hermitian transpose, respectively.

II. System Model

We take Global Positioning System (GPS) as our target application system. Consider the wavefield generated by K rays located at $\boldsymbol{\theta}$ with corresponding time delay $\boldsymbol{\tau}$, where $\boldsymbol{\theta} = [\theta_1, \ldots, \theta_K]^T$ and $\boldsymbol{\tau} = [\tau_1, \ldots, \tau_K]^T$. Under the narrowband approximation, the vector $\boldsymbol{y}(t)$ at the output of an M_θ elements array for one specific satellite signal can be represented as

$$\boldsymbol{y}(t) = \sum_{k=1}^{K} \gamma_k \boldsymbol{a}(\theta_k) c(t-\tau_k) + \boldsymbol{e}(t) \tag{1}$$

where $y(t) \doteq [y_1(t), \ldots, y_{M_\theta}(t)]^T$. $\boldsymbol{a}(\theta_k)$ and γ_k are the steering vector and the amplitude of kth ray, respectively. The $c(t-\tau_k)$ denotes the kth ray within known signal waveform $c(t)$ of C/A code and unknown delay τ_k. $\boldsymbol{e}(t) \doteq [e_1(t), \ldots, e_{M_\theta}(t)]^T$ is the Gaussian noise contribution, uncorrelated with the signals. In this paper, we assume that the number of rays is already known.

The spatial observations are collected along N periods of C/A codes with L samples in each period. Thus, the samples of the nth period of the observation interval lead to

$$\boldsymbol{Y}_b(n) \doteq [\boldsymbol{y}(((n-1)L+1)T_s), \ldots, \boldsymbol{y}(((n-1)L+L)T_s)] \tag{2}$$

where T_s is the sample interval and $l = 1, \ldots, L$, $n = 1, \ldots N$. Likewise, the sampled and shifted waveform is

$$\boldsymbol{c}(\tau_k) \doteq [c(T_s-\tau_k), \ldots, c(LT_s-\tau_k)]^T. \tag{3}$$

The computation of the parameters in (1) is complicated due to the length of sequence and sampling interval. To reduce the data amount, we compress the received signal $\boldsymbol{Y}_b(n)$ in the temporal domain. The compression can be expressed by multiplying the received signal with a correlator bank matrix $\boldsymbol{B} \in \mathbb{C}^{M_\tau \times L}$ and then by vectorizing the results we get $\boldsymbol{y_s}[n] \in \mathbb{C}^{M_\theta M_\tau \times 1}$,

$$\begin{aligned} \boldsymbol{y}_s(n) &= vec(\boldsymbol{Y}_b(n) \cdot \boldsymbol{B}^H) \\ &= \left(\boldsymbol{A}(\boldsymbol{\theta}) \otimes \boldsymbol{R}^T(\boldsymbol{\tau}, \bar{\boldsymbol{\tau}})\right) \boldsymbol{\gamma}_s + \boldsymbol{e}_s(n) \end{aligned} \tag{4}$$

with $r(\tau_k, \bar{\tau}_{m_\tau}) \doteq \boldsymbol{c}^H(\tau_k)\, \boldsymbol{c}(\bar{\tau}_{m_\tau})$, $k = 1, \ldots, K$, $m_\tau = 1, \ldots, M_\tau$ being the element of the matrix $\boldsymbol{R}(\boldsymbol{\tau}, \bar{\boldsymbol{\tau}}) \in \mathbb{C}^{K \times M_\tau}$ and the array manifold matrix defined as $\boldsymbol{A}(\theta) \doteq [\boldsymbol{a}(\theta_1), \ldots, \boldsymbol{a}(\theta_K)]$. The matrix $\boldsymbol{B}$ correlates the received signal $\boldsymbol{B} \doteq [\boldsymbol{c}(\bar{\tau}_1), \ldots, \boldsymbol{c}(\bar{\tau}_{M_\tau})]^T$ with M_τ replicas of $\boldsymbol{c}(\tau)$ with different delays $\bar{\tau}_{m_\tau}$. The set of the delay $\bar{\boldsymbol{\tau}}$ is uniformly distributed around the peak of the correlation function.

To exploit the sparsity in both spatial and temporal domains, we could extend $\boldsymbol{y}_s(n)$ into a joint two dimensional spatial and temporal sparse model by using the concept of sparse representation. According to the unequal treatment of both spatial and temporal domains, we come up with a joint on-grid DOA and off-grid delay sparse model.

Let $\tilde{\boldsymbol{\theta}} \doteq \left[\tilde{\theta}_1, \ldots, \tilde{\theta}_{N_\theta}\right]$ be the uniformly fixed sampling spatial grids with fixed DOA interval r_θ in the range $[-90°, 90°]$, similarly, for the time delay, let $\tilde{\boldsymbol{\tau}} \doteq [\tilde{\tau}_1, \ldots, \tilde{\tau}_{N_\tau}]$ be the uniformly fixed sampling time grids with fixed delay interval r_τ in the range $[-T_c, T_c]$ where T_c denotes the time duration per C/A code. As for off-grid parameters vector, $\boldsymbol{\beta_\tau} \doteq [\beta_1, \ldots, \beta_{N_\tau}]^T$ is designed where $\beta_{n_\tau} \doteq \tau_k - \tilde{\tau}_{n_{\tau k}}$ is assumed to be uniformly distributed in the interval $\left[-\frac{1}{2}r_\tau, \frac{1}{2}r_\tau\right]$, with $\tilde{\tau}_{n_{\tau k}}$ being the nearest grid to the kth signal. Thus, we can construct an on-grid DOA and off-grid delay over complete basis matrix

$$\boldsymbol{\Phi}(\boldsymbol{\beta}_\tau) = \boldsymbol{A} \otimes (\boldsymbol{C} + \boldsymbol{B}_\tau \mathrm{diag}(\boldsymbol{\beta}_\tau)) \tag{5}$$

where $\boldsymbol{A} = \left[\boldsymbol{a}\left(\tilde{\theta}_1\right), \ldots, \boldsymbol{a}\left(\tilde{\theta}_{N_\theta}\right)\right] \in \mathbb{C}^{M_\theta \times N_\theta}$. $\boldsymbol{C} \in \mathbb{C}^{M_\tau \times N_\tau}$ is composed of the element $r(\bar{\tau}_{m_\tau}, \tilde{\tau}_{n_\tau})$ with $m_\tau = 1, \ldots, M_\tau$, $n_\tau = 1, \ldots, N_\tau$. $\boldsymbol{B}_\tau \in \mathbb{C}^{M_\tau \times N_\tau}$ is the first order Taylor series expansion derivation of $b(\bar{\tau}_{m_\tau}, \tilde{\tau}_{n_\tau}) \doteq \frac{\partial r(\bar{\tau}_{m_\tau}, \tilde{\tau}_{n_\tau})}{\partial \tilde{\tau}_{n_\tau}}$.

By extending to multiple measurement vectors model, denote the matrices $\boldsymbol{Y} \doteq [\boldsymbol{y}_s(1), \ldots, \boldsymbol{y}_s(N)] \in \mathbb{C}^{M_\theta M_\tau \times N}$ and $\boldsymbol{E} \doteq [e_s(1), \ldots, e_s(N)] \in C^{M_\theta M_\tau \times N}$, then the joint on-grid DOA and off-grid delay estimation sparse model becomes

$$\boldsymbol{Y} = \boldsymbol{\Phi}(\boldsymbol{\beta}_\tau) \boldsymbol{X} + \boldsymbol{E} \tag{6}$$

with complex source amplitudes $\boldsymbol{X} = [\boldsymbol{x}_s[1], \ldots, \boldsymbol{x}_s[N]] \in \mathbb{C}^{N_\theta N_\tau \times N}$ that only few of them are zero. The matrix $\boldsymbol{X}$ of interest is sparse that all the columns of $\boldsymbol{X}$ are sparse and share the same support.

III. Existing Methods

In this section, two typical methods, SAGE and MUSIC for spatial and temporal estimation are briefly reviewed in GNSS multipath environment.

A. Spatial and Temporal Estimation based on SAGE

SAGE iteratively approximates the ML estimator and has been successfully applied for parameter estimation in GNSS [5]. The core idea of SAGE is performing a sequence of maximization steps in spaces of lower dimension.

Denote $\boldsymbol{s}_k(t) \doteq \gamma_k \boldsymbol{a}(\theta_k) c(t-\tau_k)$ in (1). Thus, we get the sampled $\boldsymbol{S}_{b,k}$ and $\boldsymbol{E}_{b,k}$ for each ray. Follow the introductions in [4] and [5], SAGE can be implemented by two main steps. The one expectation step is

$$\hat{\boldsymbol{X}}_{b,k} = \boldsymbol{Y}_b - \sum_{k'=1, k' \neq k}^{K} \boldsymbol{S}_{b,k'}. \tag{7}$$

Then the following step is maximization,

$$\hat{\theta}_k = \arg\max_{\theta_k} \left\{ \left| \boldsymbol{a}^H(\theta_k) \hat{\boldsymbol{X}}_{b,k} \boldsymbol{c}(\hat{\tau}_k)^H \right|^2 \right\} \tag{8}$$

$$\hat{\tau}_k = \arg\max_{\tau_k} \left\{ \left| \boldsymbol{a}^H\left(\hat{\theta}_k\right) \hat{\boldsymbol{X}}_{b,k} \boldsymbol{c}(\tau_k)^H \right|^2 \right\}. \tag{9}$$

Obviously, SAGE is quite sensitive to initialization due to (7).

B. Spatial and Temporal Estimation based on MUSIC

MUSIC is a promising super-resolution subspace-based method and was proposed by extending the geometric concepts to obtain a reasonable approximate solution in the presence of noise. In this paper, the joint angle and delay estimation based on MUSIC is implemented on model (4).

Nevertheless, MUSIC is not the proper algorithm in multipath discrimination. To conquer this problem, spatial s-moothing [16] is applied as well by forming the submatrix $\boldsymbol{U}_m \doteq \boldsymbol{\Psi}_J \left(\boldsymbol{A}(\boldsymbol{\theta}) \otimes \boldsymbol{R}^H(\boldsymbol{\tau}, \bar{\boldsymbol{\tau}})\right)$ where $\boldsymbol{\Psi}_J \doteq [\boldsymbol{I}_J, \boldsymbol{0}_{J,M_\theta-J}]$. So the $M_\theta - J + 1$ groups could be gathered by sliding

$$\boldsymbol{T}_s \doteq \boldsymbol{U}_m \left[\boldsymbol{I}\boldsymbol{\gamma}_s, \boldsymbol{\Phi}_s\boldsymbol{\gamma}_s, \ldots, \boldsymbol{\Phi}_s^{M_\theta-J+1}\boldsymbol{\gamma}_s\right] + \boldsymbol{E}_s \tag{10}$$

where $\boldsymbol{\Phi}_s = \mathrm{diag}\left\{e^{jd\sin(\theta_1)}, \ldots, e^{jd\sin(\theta_K)}\right\}$ is the phase difference matrix contributing to resolving the multipath signals. By taking the noise subspace $\hat{\mathbf{U}}_N$ via eigen-decomposition of $\boldsymbol{T}_s\boldsymbol{T}_s^H$, we could search the parameters with the spectrum

$$\left\{\hat{\boldsymbol{\theta}}, \hat{\boldsymbol{\tau}}\right\} = \arg\max_{\theta,\tau}\left\{\frac{1}{\boldsymbol{U}_m^H\hat{\boldsymbol{U}}_N\hat{\boldsymbol{U}}_N^H\boldsymbol{U}_m}\right\}. \tag{11}$$

IV. Spatial and Temporal Estimation based on MSBL

In this paper, a sparse Bayesian rules based method is proposed to settle the multipath resolvation using model (6). The problem at hand of the joint on-grid DOA and off-grid delay estimation is converted to find not only the set of non-zero indices of the matrix $\boldsymbol{X}$ but also the off-grid parameters vector $\boldsymbol{\beta}_\tau$ for delay. To realize the JAODE-MSBL algorithm, the distribution assumptions are given as follows.

We assume that the additive noise in (6) is complex Gaussian noise with variance σ^2 and zero mean value. When σ^2 is assumed to be unknown, by defining a hyperparameter, i.e., the precision, $\alpha_n \triangleq \sigma^{-2}$. Then we have

$$\begin{aligned} &p\left(\boldsymbol{Y}\left|\boldsymbol{X}, \alpha_n, \boldsymbol{\beta}_\tau\right.\right) \\ &= \prod_{n=1}^{N} \mathcal{CN}\left(\boldsymbol{y}_s(n)\left|\boldsymbol{\Phi}(\boldsymbol{\beta}_\tau)\boldsymbol{x}_s(n)\right., \alpha_n^{-1}\boldsymbol{I}_{M_\theta,M_\tau}\right) \end{aligned} \tag{12}$$

and a Gamma distribution is used to describe the inverse of noise variance

$$p(\alpha_n; a, b) = \mathcal{B}\left(\alpha_n | a, b\right) \tag{13}$$

where $\mathcal{B}\left(\alpha_n | a, b\right) \doteq [\Gamma(a)]^{-1} b^a \alpha_n^{a-1} e^{-b\alpha_n}$ with the Gamma function $\Gamma(a) \doteq \int_0^\infty x^{a-1}e^{-x}dx$. a and b are the hyperparameters for α_n.

For the prior of complex source amplitudes $\boldsymbol{X}$, it can be seen as independent both across C/A codes and space-time domain, which follows a zero-mean complex Gaussian distribution with DOA-delay-dependent variance $\boldsymbol{\alpha} = [\alpha_1, \ldots, \alpha_{N_\theta N_\tau}]^T$ and $\boldsymbol{\Upsilon} = \mathrm{diag}(\boldsymbol{\alpha})$,

$$p(\boldsymbol{X}|\boldsymbol{\alpha}) = \prod_{n=1}^{N} \mathcal{CN}\left(\boldsymbol{x}_s[n] | 0, \boldsymbol{\Upsilon}\right). \tag{14}$$

A two-stage hierarchical prior is adopted here which favors most rows of $\boldsymbol{X}$ being zeros

$$p(\boldsymbol{\alpha}, \rho) = \prod_{n_g=1}^{N_\theta N_\tau} \Gamma\left(\boldsymbol{\alpha}(n_g) | 1, \rho\right). \tag{15}$$

For the off-grid parameter vector $\boldsymbol{\beta}_\tau$, a non-informative uniform prior is used

$$p(\boldsymbol{\beta}_\tau; r_\tau) = U\left(\left[-\frac{1}{2}r_\tau, \frac{1}{2}r_\tau\right]\right) \tag{16}$$

where we have

$$U([c,d]) = \begin{cases} \frac{1}{d-c}, & c \le x \le d \\ 0, & otherwise. \end{cases} \tag{17}$$

To estimate DOAs and delays, we can formulate the following problem to maximize the posterior probability with the received signal

$$\begin{aligned} &\left\{\hat{\boldsymbol{X}}, \hat{\alpha}_n, \hat{\boldsymbol{\alpha}}, \hat{\boldsymbol{\beta}}_\tau\right\} \\ &= \arg\max_{\{\boldsymbol{X},\alpha_n,\boldsymbol{\alpha},\boldsymbol{\beta}_\tau\}} p\left(\boldsymbol{X}, \alpha_n, \boldsymbol{\alpha}, \boldsymbol{\beta}_\tau \left|\boldsymbol{Y}\right.\right). \end{aligned} \tag{18}$$

However, the problem of posterior probability above cannot be solved directly, so an EM method is adopted to realize SBL. To obtain the posterior distribution of $\boldsymbol{X}$, we first calculate the joint distribution for all parameters

$$\begin{aligned} &p\left(\boldsymbol{X}, \boldsymbol{Y}, \alpha_n, \boldsymbol{\alpha}, \boldsymbol{\beta}_\tau\right) \\ &= p\left(\boldsymbol{Y}\left|\boldsymbol{X}, \alpha_n, \boldsymbol{\beta}_\tau\right.\right) p\left(\boldsymbol{X}|\boldsymbol{\alpha}\right) p(\boldsymbol{\alpha}) p(\alpha_n) p(\boldsymbol{\beta}_\tau). \end{aligned} \tag{19}$$

The posterior for $\boldsymbol{X}$ can be obtained as

$$p\left(\boldsymbol{X}\left|\boldsymbol{Y}; \alpha_n, \boldsymbol{\alpha}, \boldsymbol{\beta}_\tau\right.\right) \propto p\left(\boldsymbol{Y}\left|\boldsymbol{X}; \alpha_n, \boldsymbol{\beta}_\tau\right.\right) p(\boldsymbol{X}|\boldsymbol{\alpha}). \tag{20}$$

After a simple derivation, their product (20) is also Gaussian with posterior mean value $\boldsymbol{\mu}_x$ and covariance $\boldsymbol{\Sigma}_x$

$$\boldsymbol{\mu}_x(n) = \alpha_n \boldsymbol{\Sigma}_x \boldsymbol{\Phi}^H(\boldsymbol{\beta}_\tau)\boldsymbol{y}_s(n) \tag{21}$$

$$\boldsymbol{\Sigma}_x = \left(\alpha_n \boldsymbol{\Phi}^H(\boldsymbol{\beta}_\tau)\boldsymbol{\Phi}(\boldsymbol{\beta}_\tau) + \boldsymbol{\Upsilon}^{-1}\right)^{-1} \tag{22}$$

where $n = 1, \ldots, N$.

From the formulations mentioned above, hyperparameters α_n, $\boldsymbol{\alpha}$, $\boldsymbol{\beta}_\tau$ are needed to be known when calculate $\boldsymbol{\mu}_x$ and $\boldsymbol{\Sigma}_x$. To address the hyperparameters estimate, an expectation maximization algorithm is implemented that treats $\boldsymbol{X}$ as a hidden variable and turns to maximizing $E\{p(\boldsymbol{X}, \boldsymbol{Y}, \alpha_n, \boldsymbol{\alpha}, \boldsymbol{\beta}_\tau)\}$. Following a similar procedure as in [14] denoting $\boldsymbol{U} = [\boldsymbol{u}_x(1), \ldots, \boldsymbol{u}_x(N)]$, it is easy to obtain the following updates of $\boldsymbol{\alpha}$ and σ^2 by maximizing $E\{\ln p(\boldsymbol{X}|\boldsymbol{\alpha})p(\boldsymbol{\alpha})\}$ and $E\{\ln p(\boldsymbol{Y}|\boldsymbol{X}, \alpha_n, \boldsymbol{\alpha}, \boldsymbol{\beta}_\tau)p(\alpha_n)\}$,

$$\boldsymbol{\alpha}(n_g) = \frac{\sqrt{N^2 + 4\rho E\left\{\|\boldsymbol{X}(n_g,:)\|_2^2\right\}} - 1}{2\rho} \tag{23}$$

$$\alpha_n = \frac{M_\theta M_\tau \cdot N + a - 1}{E\left\{\|\boldsymbol{Y} - \boldsymbol{\Phi}(\boldsymbol{\beta}_\tau)\boldsymbol{X}\|_F^2\right\} \cdot N + b} \tag{24}$$

where $E\left\{\left\|\boldsymbol{X}\left(n_g,:\right)\right\|_2^2\right\} = \left\|\boldsymbol{U}\left(n_g,:\right)\right\|_2^2 + \boldsymbol{\Sigma}\left(n_g,n_g\right)$ and $E\left\{\left\|\boldsymbol{Y}-\boldsymbol{\Phi}\boldsymbol{X}\right\|_F^2\right\} = \left\|\boldsymbol{Y}-\boldsymbol{\Phi}\boldsymbol{U}\right\|_F^2 + \boldsymbol{\alpha}\left(n_g\right)\sum_{n=1}^{N_\theta N_\tau}\varsigma\left(n_g\right)$ with $\varsigma\left(n_g\right) = 1 - \boldsymbol{\alpha}^{-1}\left(n_g\right)\boldsymbol{\Sigma}\left(n_g,n_g\right)$, $n_g = 1,\ldots,N_\theta N_\tau$.

Referring to the off-grid parameter vector $\boldsymbol{\beta}_\tau$, $E\left\{\log p\left(\boldsymbol{Y}\left|\boldsymbol{X},\sigma^2,\boldsymbol{\beta}_\tau\right.\right)p\left(\boldsymbol{\beta}_\tau\right)\right\}$ is the part related to (18) that its estimate maximizes and thus minimizes

$$\begin{aligned}&E\left\{\frac{1}{N}\sum_{n=1}^{N}\left\|\boldsymbol{y}_s\left(n\right)-\boldsymbol{\Phi}\left(\boldsymbol{\beta}_\tau\right)\boldsymbol{x}_s\left(n\right)\right\|_2^2\right\}\\&=\frac{1}{N}\sum_{n=1}^{N}\left\|\boldsymbol{y}_s(n)-\boldsymbol{\Phi}(\boldsymbol{\beta}_\tau)\boldsymbol{\mu}_x(n)\right\|_2^2+Tr\left\{\boldsymbol{\Phi}(\boldsymbol{\beta}_\tau)\boldsymbol{\Sigma}_x\boldsymbol{\Phi}^H(\boldsymbol{\beta}_\tau)\right\}\\&=\boldsymbol{\beta}_\tau^T\boldsymbol{P}_\tau\boldsymbol{\beta}_\tau-2\boldsymbol{v}_\tau^T\boldsymbol{\beta}_\tau+C_1\end{aligned} \tag{25}$$

where C_1 is a constant term independent of $\boldsymbol{\beta}_\tau$. $\boldsymbol{P}_\tau$ is a positive semi-definite matrix

$$\begin{aligned}\boldsymbol{P}_\tau=&\Re\left\{\frac{1}{N}\sum_{n=1}^{N}\boldsymbol{\Xi}(n)^H\boldsymbol{\Xi}\left(n\right)\right\}\\&+\Re\left\{\boldsymbol{J}_1^T\left(\boldsymbol{\Sigma}_x\odot\left(\boldsymbol{A}\otimes\boldsymbol{B}_\tau\right)^H\left(\boldsymbol{A}\otimes\boldsymbol{B}_\tau\right)\right)\boldsymbol{J}_1\right\}\end{aligned} \tag{26}$$

$$\begin{aligned}\boldsymbol{v}_\tau=&\Re\left\{\frac{1}{N}\sum_{n=1}^{N}\left\{\left(\boldsymbol{y}_s\left(n\right)-\left(\boldsymbol{A}\otimes\boldsymbol{C}\right)\boldsymbol{\mu}_x\left(n\right)\right)^H\boldsymbol{\Xi}\left(n\right)\right\}\right\}^T\\&-\Re\left\{\left\{\operatorname{diag}\left(\left(\boldsymbol{A}^H\boldsymbol{A}\otimes\boldsymbol{B}_\tau^H\boldsymbol{C}\right)\boldsymbol{\Sigma}_x\right)\right\}^T\boldsymbol{J}_1\right\}^T\end{aligned} \tag{27}$$

with $\boldsymbol{\Xi}\left[n\right] = \left(\left(\boldsymbol{A}mat\boldsymbol{\mu}_x^T\left(n\right)\right)\otimes\boldsymbol{I}_{M_\tau}\right)\left(\boldsymbol{I}_{N_\tau}\otimes\boldsymbol{B}_\tau\right)\boldsymbol{J}_2$. In the above equations, both of $\boldsymbol{J}_1$ and $\boldsymbol{J}_2$ are selection matrix. $\boldsymbol{J}_1 \in \mathbb{C}^{N_\theta N_\tau\times N_\tau}$ is arranged by column of $\boldsymbol{N}_\theta$ unit diagonal matrix $\boldsymbol{I}_{N_\tau}$. $\boldsymbol{J}_2 \in \mathbb{C}^{N_\tau^2\times N_\tau}$ is a known matrix with the element of $N_\tau\left(m_\tau-1\right)+m_\tau\,\mathrm{th}$ row and $m_\tau\,\mathrm{th}$ column being one, $m_\tau = 1,\ldots,N_\tau$, and other elements are zero. $mat\boldsymbol{\mu}_x\left(n\right)\in\mathbb{C}^{N_\tau\times N_\theta}$ is a reshaped matrix of colomn vector $\boldsymbol{\mu}_x\left(n\right)$. Besides, the derivation above of details is shown in Appendix.

As a result, we have

$$\hat{\boldsymbol{\beta}}_\tau = \arg\min_{\boldsymbol{\beta}_\tau\in\left[-\frac{1}{2}r_\tau,\frac{1}{2}r_\tau\right]}\left\{\boldsymbol{\beta}_\tau^T\boldsymbol{P}\boldsymbol{\beta}_\tau-2\boldsymbol{v}^T\boldsymbol{\beta}_\tau\right\} \tag{28}$$

for the purpose of estimating the off-grid parameter vector. The JAODE-MSBL algorithm is concluded as follows.

JAODE-MSBL algorithm

1: ***Initialization***: $\alpha_n = 100/var\left\{\boldsymbol{Y}\right\}$, $\boldsymbol{\beta}_\tau = \boldsymbol{0}$ and $\boldsymbol{\alpha} = \left(\boldsymbol{\Phi}^H\boldsymbol{Y}\right)/\left(M_\theta M_\tau\left(M_\theta M_\tau-1\right)\right)$. The hyperparameters $a = b = 1\times10^{-4}$ and $\rho = 0.01$.
2: ***Repeat***
3: **Calculate** $\boldsymbol{\Sigma}_x$, $\boldsymbol{\mu}_x$ and $\boldsymbol{\Phi}\left(\boldsymbol{\beta}_\tau\right)$ using the current values of the hyperparameters according to (22), (21) and (5), respectively;
4: **Update** $\boldsymbol{\alpha}$ and σ^2 according to (23) and (24);
5: **Find** the K largest peaks in $\boldsymbol{\alpha}$ and calculate the corresponding DOA and delay on-grid number, respectively;
6: **Update** $\boldsymbol{\beta}_\tau$ according to (26) - (28);
7: **Calculate** the error $\varepsilon = \left\|\boldsymbol{\alpha}^{new}-\boldsymbol{\alpha}^{old}\right\|_2/\left\|\boldsymbol{\alpha}^{old}\right\|_2$.
8: ***Until***(convergence $\varepsilon \le 10^{-3}$ or iterations $\le$ 500).

V. Numerical Results

In this paper, we compare the proposed algorithm JAODE-MSBL with the existing methods, such as the SAGE and spatial smoothing JADE-MUSIC (SS-JADE-MUSIC) reviewed in the former sections for various GNSS multipath scenarios.

For the JAODE-MSBL algorithm, the specific settings are listed below. The scanning DOA grid is uniformly distributed in the range from $-90°$ to $90°$ with the DOA interval $r_\theta = 2°$ between adjacent grid points. With the uniform scanning delay grid range from $-2T_c$ to $2T_c$, the delay interval between adjacent grid points is $r_\tau = 0.1T_c$.

Unless noted otherwise, SAGE is implemented by two different initializations: the ideal one (SAGEi) and the practical one (SAGEp). The former one is that both DOA and delay are initialized randomly within $(-1.5°, 1.5°)$ and $(-0.075T_c, +0.075T_c)$ biases for two paths, respectively. The latter is set more reasonable that the initial DOAs are unknown when searching and the time delay of main path is known acquired by acquisition.

For SS-JADE-MUSIC, the sliding elements of arrays is $J = 6$.

For simplicity, we assume a uniform linear array (ULA) with $M_d = 8$ sensors and half-wavelength interelement spacing. There are 10ms C/A codes in total. The sampling rate is $P = 4$. Here we consider two paths in total $(K = 2)$: a LOSS and a single reflective multipath. The direct to multipath ratio is 0.8.

With the $N_l = 1000$ trials, the root mean square error $\mathrm{RMSE}\left(\tau_1\right) = \sqrt{\frac{1}{N_l}\sum_{n_l=1}^{N_l}\left(\hat{\tau}_1-\tau_1\right)^2}$ is measured the LOSS estimation performance.

A. Scenario A: low spatially correlated rays

In this scenario, we consider the LOSS and the multipath are separable in spatial domain. These two correlated rays are separated by DOA θ_1, θ_2 at $-0.7°$ and $30.2°$, with corresponding delay τ_1, τ_2 being $0.03T_c$ and $0.38T_c$, respectively.

As shown in Fig. 1 and 2, both 2D-SAGE and SS-JADE-MUSIC achieve the best performances in high C/N_0 in case of low spatially correlated rays. However, with low C/N_0 the DOAs and delays cannot be estimated correctly by 2D-SAGEp and SS-JADE-MUSIC. On the contrary, JAODE-MUSIC becomes a little bit flat in high C/N_0 both in DOA and delay estimation yet with different reasons: on-grid estimation and first-order Taylor series expansion, respectively. When in lower C/N_0, JAODE-MSBL is more appropriate to GNSS receiver than others due to the fact that most of the typical GNSS signals are located in the region from 35 dB-Hz to 55 dB-Hz.

B. Scenario B: highly spatially correlated rays

In order to get a deep insight about the performances of proposed method in highly spatially correlated case, the DOAs θ_1, θ_2 of the LOSS and the multipath signal are set to $0.3°$ and $6.8°$, respectively, while the delays τ_1, τ_2 remain $0.03T_c$ and $0.38T_c$.

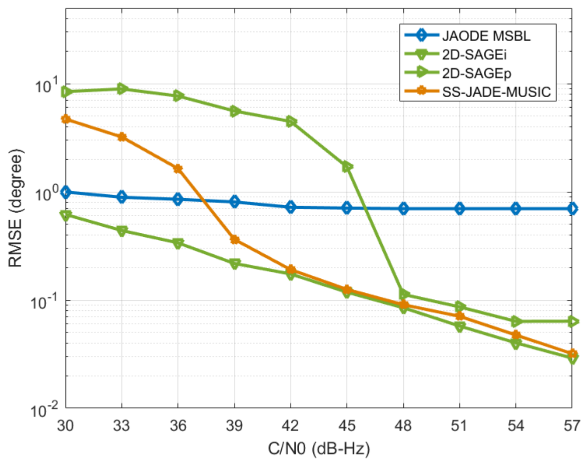

Fig. 1. RMSE of the DOA for scenario A

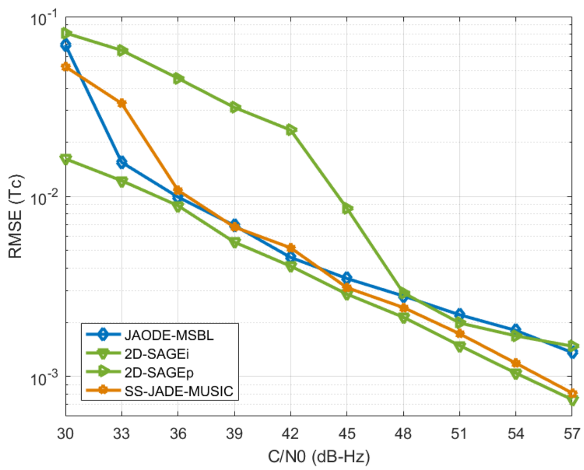

Fig. 2. RMSE of the time delay for scenario A

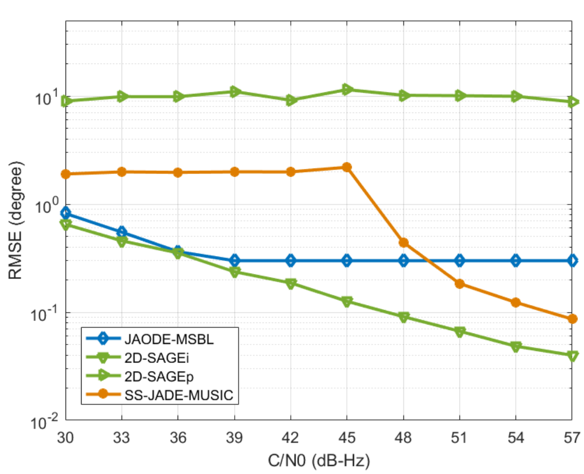

Fig. 3. RMSE of the DOA for scenario B

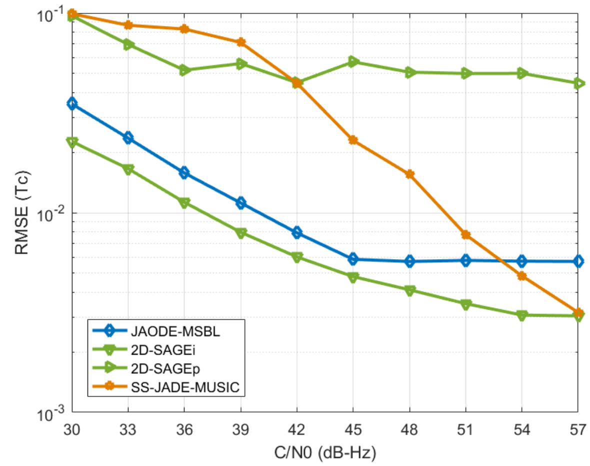

Fig. 4. RMSE of the time delay for scenario B

In comparison to scenario A, highly spatially correlated rays lead to the fact that neither 2D-SAGEp or SS-JADE-MUSIC works well. Even 2D-SAGEi cannot resolve the two paths thoroughly in high C/N_0. However, JAODE-MSBL algorithm has a strong robustness against multipath as shown in Fig.3 and 4. It particularly performs as good as 2D-SAGEi in delay estimation, even reaching the level of $10^{-2}T_c$, the decimeter level, at only 40 dB-Hz.

C. *Scenario C: highly temporally correlated rays*

We will be continuing to explore the performance of proposed method in a highly temporally correlated case, the DOAs θ_1, θ_2 of the LOSS and the multipath signal are set to be $0.3°$, $10.8°$, while the delays τ_1, τ_2 are narrowed to $0.03T_c$ and $0.13T_c$, respectively.

In both highly spatially and temporally correlated rays scenarios, the performance of 2D-SAGEp continues to deteriorate, especially in low C/N_0. Meanwhile, SS-JADE-MUSIC performs better than it in Scenario B due to the spatial smoothing. Even though 2D-SAGEi is good to see under 48 dB-Hz, it becomes flat in high C/N_0 which confirms that SAGE cannot discriminate two highly temporally correlated rays anymore in high C/N_0. Conversely, JAODE-MSBL performs well after 42 dB-Hz showing that it can provide the accurate values.

VI. Conclusion

The joint DOA and delay estimation problem for multipath mitigation in GNSS has been investigated in this paper. The novel JAODE-MSBL algorithm has been proposed to estimate on-grid DOA and off-grid delay which reduces the complexity and enhances the resolution. Simulation results confirm that the proposed JAODE-MSBL provides more accuracy delay estimation and outperforms in multipath discrimination especially in low C/N_0 and spatially correlated rays. However, different GNSS scenarios acquire different MSBL based estimators. Future work will focus on the extended derivation of the proposed algorithm in adaption to various GNSS scenarios.

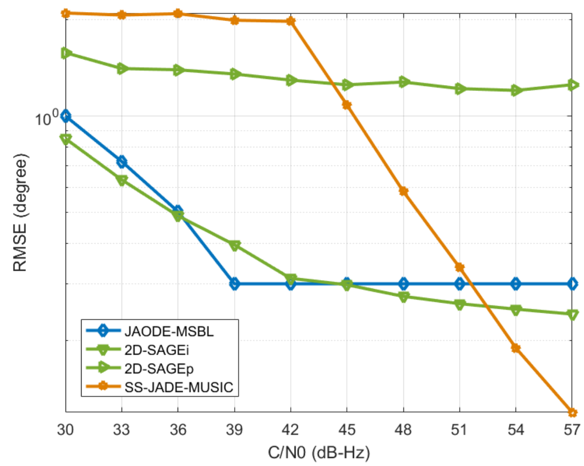

Fig. 5. RMSE of the DOA for scenario C

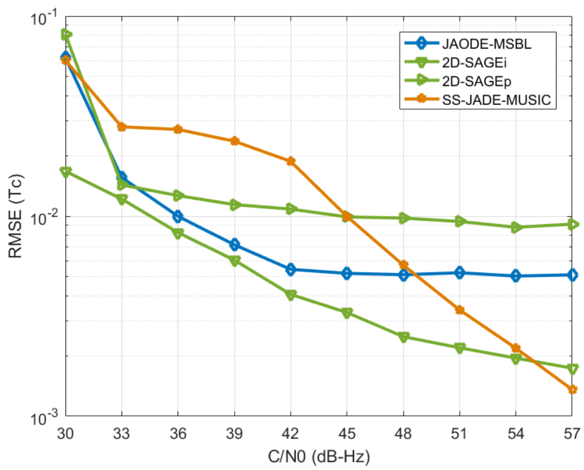

Fig. 6. RMSE of the time delay for scenario C

Appendix

Define (20) into two parts and we calculate them separately where the sampling point t here is omitted for short

$$\begin{aligned} F_A &= \|\boldsymbol{y}_s - [\boldsymbol{A} \otimes (\boldsymbol{C} + \boldsymbol{B}_\tau diag(\boldsymbol{\beta}_\tau))] \boldsymbol{\mu}_x\|_2^2 \\ &= \left\|\boldsymbol{y}_s - (\boldsymbol{A} \otimes \boldsymbol{C}) \boldsymbol{\mu}_x - vec\left((\boldsymbol{B} diag(\boldsymbol{\beta}_\tau)) mat \boldsymbol{\mu}_x \boldsymbol{A}^T\right)\right\|_2^2 \\ &= \|\boldsymbol{y}_s - (\boldsymbol{A} \otimes \boldsymbol{C}) \boldsymbol{\mu}_x - \boldsymbol{\Xi}\boldsymbol{\beta}_\tau\|_2^2 \\ &= -2\Re\left\{(\boldsymbol{y}_s - (\boldsymbol{A} \otimes \boldsymbol{C}) \boldsymbol{\mu}_x)^H \boldsymbol{\Xi}\right\} \boldsymbol{\beta}_\tau + \boldsymbol{\beta}_\tau^T \boldsymbol{\Xi}^H \boldsymbol{\Xi} \boldsymbol{\beta}_\tau + C_2 \end{aligned} \tag{29}$$

$$\begin{aligned} F_B &= Tr\left\{\boldsymbol{\Phi}(\boldsymbol{\beta}_\tau) \boldsymbol{\Sigma}_x \boldsymbol{\Phi}(\boldsymbol{\beta}_\tau)^H\right\} \\ &= 2\Re\left\{Tr\left\{(\boldsymbol{A} \otimes \boldsymbol{C}) \boldsymbol{\Sigma}_x (\boldsymbol{A} \otimes (\boldsymbol{B}_\tau diag(\boldsymbol{\beta}_\tau)))^H\right\}\right\} \\ &+ Tr\left\{(\boldsymbol{A} \otimes (\boldsymbol{B}_\tau diag(\boldsymbol{\beta}_\tau))) \boldsymbol{\Sigma}_x (\boldsymbol{A} \otimes (\boldsymbol{B}_\tau diag(\boldsymbol{\beta}_\tau)))^H\right\} \\ &+ C_3 \end{aligned} \tag{30}$$

where C_2, C_3 are the parts irrelevant to $\boldsymbol{\beta}_\tau$. Then split F_B into two parts for simplicity,

$$\begin{aligned} F_C &= \Re\left\{Tr\left\{(\boldsymbol{A} \otimes \boldsymbol{C}) \boldsymbol{\Sigma}_x (\boldsymbol{A} \otimes (\boldsymbol{B}_\tau diag(\boldsymbol{\beta}_\tau)))^H\right\}\right\} \\ &= \Re\left\{Tr\left\{\left(\boldsymbol{A}^H \boldsymbol{A} \otimes \boldsymbol{B}^H \boldsymbol{C}\right) \boldsymbol{\Sigma}_x diag(\boldsymbol{J}_1 \boldsymbol{\beta}_\tau)\right\}\right\} \\ &= \Re\left\{diag\left(\left(\boldsymbol{A}^H \boldsymbol{A} \otimes \boldsymbol{B}^H \boldsymbol{C}\right) \boldsymbol{\Sigma}_x\right)\right\}^T (\boldsymbol{J}_1 \boldsymbol{\beta}_\tau) \end{aligned} \tag{31}$$

$$\begin{aligned} F_D &= Tr\left\{(\boldsymbol{A} \otimes (\boldsymbol{B} diag(\boldsymbol{\beta}_\tau))) \boldsymbol{\Sigma}_x (\boldsymbol{A} \otimes (\boldsymbol{B} diag(\boldsymbol{\beta}_\tau)))^H\right\} \\ &= \boldsymbol{\beta}_\tau^T \boldsymbol{J}_1^T \left(\boldsymbol{\Sigma}_x \odot (\boldsymbol{A} \otimes \boldsymbol{B})^H (\boldsymbol{A} \otimes \boldsymbol{B})\right) \boldsymbol{J}_1 \boldsymbol{\beta}_\tau. \end{aligned} \tag{32}$$

Follow the above equations, $\boldsymbol{P}_\tau$ and $\boldsymbol{v}_\tau$ are acquired. Note that $\boldsymbol{\beta}_\tau^T \boldsymbol{Q} \boldsymbol{\beta}_\tau$ belongs to real domain under the circumstance of a positive semi-definite matrix $\boldsymbol{Q}$ thus leads a result $\boldsymbol{\beta}_\tau^T \boldsymbol{Q} \boldsymbol{\beta}_\tau = \Re\left\{\boldsymbol{\beta}_\tau^T \boldsymbol{Q} \boldsymbol{\beta}_\tau\right\} = \boldsymbol{\beta}_\tau^T \Re\{\boldsymbol{Q}\} \boldsymbol{\beta}_\tau$ due to the real-valued $\boldsymbol{\beta}_\tau$. Then we have the positive semi-definite matrix $\boldsymbol{P}_\tau$.

References

[1] V. Nee, R. DJ, "Multipath effects on GPS code phase measurements," Navigation, vol. 39, pp. 177–190, 1992.

[2] M. Maqsood, S. Gao, T. Brown, and M. Unwin, "Effects of ground plane on the performance of multipath mitigating antennas for GNSS," 2010 Loughborough Antennas & Propagation Conference, vol. A247, pp. 241–244, 2010.

[3] G. Seco Granados, "Antenna arrays for multipath and interference mitigation in GNSS receivers," Universitat Politècnica de Catalunya, 2000.

[4] B. H.Fleury, M. Tschudin, R. Heddergott, D. Dahlhaus, and K. Ingeman Pedersen, "Channel parameter estimation in mobile radio environments using the SAGE algorithm," IEEE Journal on selected areas in communications, vol. 17, pp. 434–450, 1999.

[5] F. Antreich, J.A. Nossek, and W. Utschick, "Maximum likelihood delay estimation in a navigation receiver for aeronautical applications," Aerospace Science and Technology, vol. 12, pp. 256–267, 2008.

[6] R. Schmidt, "Multiple emitter location and signal parameter estimation," IEEE transactions on antennas and propagation, vol. 34, pp. 276–280, 1986.

[7] R. Roy, and T. Kailath, "ESPRIT-estimation of signal parameters via rotational invariance techniques," IEEE transactions on antennas and propagation, vol. 37, pp. 984–995, 1989.

[8] M. C.Vanderveen, C. B.Papadias, and A. Paulraj, "Joint angle and delay estimation (JADE) for multipath signals arriving at an antenna array," IEEE Communications letters, vol. 1, pp. 12–14, 1997.

[9] N. Chang, X. Hong, W. Wang, and Z. Wang, "Subspace based joint delay and direction of arrival estimation for GNSS multipath signals," China Satellite Navigation Conference, pp. 189–199, 2018.

[10] N. Chang, X. Hong, W. Wang, and Z. Wang, "Joint delay and angle estimation for GNSS multipath signals based on spatial and frequential smoothing," 2018 14th IEEE International Conference on Signal Processing (ICSP), pp. 203–207, 2018.

[11] X. Hong, N. Chang, W. Wang, and Q. Yin, "Subspace-based joint DOA, delay and DFO estimation for GNSS multipath signals," Proceedings of the ION GNSS+ Meeting, 2018.

[12] S. Fortunati, R. Grasso, F. Gini, M. S Greco, and K. LePage, "Single-snapshot DOA estimation by using compressed sensing," EURASIP Journal on Advances in Signal Processing, vol.2014, pp. 120, 2014.

[13] T. Yardibi, J. Li, P. Stoica, M. Xue, and A. Baggeroer, "Source localization and sensing: A nonparametric iterative adaptive approach based on weighted least squares," IEEE Transactions on Aerospace and Electronic Systems, vol. 46, pp. 425–443, 2010.

[14] ME. Tipping, "Sparse bayesian learning and the relevance vector machine," Journal of machine learning research, vol. 1, pp. 211–244, 2001.

[15] Z. Yang, L. Xie, and C. Zhang, "Off-grid direction of arrival estimation using sparse Bayesian inference," IEEE Transactions on Signal Processing, vol. 61, pp. 38–43, 2012.

[16] SU. Pillai, BH. Kwon, "Forward/backward spatial smoothing techniques for coherent signal identification," IEEE Transactions on Acoustics, Speech, and Signal Processing, vol. 37, pp. 984–995, 1989.